

Author's post-print of the article

G.C. Sosso and M. Bernasconi, *Harnessing machine learning potentials to understand the functional properties of phase-change materials*, MRS Bulletin **44**, 705 (2019); doi:10.1557/mrs.2019.202

Harnessing machine learning potentials to understand the functional properties of phase-change materials

G.C. Sosso and M. Bernasconi

G.C. Sosso, Department of Chemistry and Centre for Scientific Computing, University of Warwick, UK; g.sosso@warwick.ac.uk

M. Bernasconi, Department of Materials Science, University of Milano-Bicocca, Italy; marco.bernasconi@unimib.it

The exploitation of phase-change materials in diverse technological applications can be greatly aided by a better understanding of the microscopic origins of their functional properties. Over the last decade, simulations based on electronic structure calculations within density functional theory (DFT) have provided useful insights into the properties of phase-change materials. However, large simulation cells and long simulation times beyond the reach of DFT simulations are needed to address several key issues of relevance for the performance of devices. One way to overcome the limitations of DFT methods is to use machine learning (ML) techniques to build interatomic potentials for fast molecular dynamics simulations that still retain a *quasi-ab initio* accuracy. Here, we review the insights gained on the functional properties of the prototypical phase-change material GeTe by harnessing such interatomic potentials. Applications and future

challenges of the ML techniques in the study of phase-change materials are also outlined.

Keywords: machine learning, memory, simulation, amorphous, crystallization

Introduction

The development of novel nonvolatile memories (NVMs) is key to further our ability to retain, share and process the ever-growing amount of data generated every day. Current NVMs based on Flash technology suffer from relatively low speeds and limited endurance. Among the alternative options to Flash technology, phase-change memories^{1,2} stand out as one of the most promising candidates, as attested to by the recent Optane memory, based on the Intel/Micron 3D Xpoint technology, that entered the market in 2017 as storage-class memories.³

In phase-change memories, information is encoded into two different phases of phase-change materials such as chalcogenide alloys,^{4,5} which can reversibly (up to $\sim 10^{12}$ times)^{6,7} switch between the crystalline and amorphous phases upon Joule heating within a few nanoseconds. The two phases have markedly different electrical resistance values that are exploited in the memory readout.

Although the $\text{Ge}_2\text{Sb}_2\text{Te}_5$ compound is presently the material of choice for phase-change memories, the quest for alloys with better performance continues.^{5,8} For embedded applications in the automotive industry, for instance, data retention above 100°C is desirable, which is not achievable with $\text{Ge}_2\text{Sb}_2\text{Te}_5$. Other applications such as neuro-inspired computing⁹ and photonic devices¹⁰ would also benefit from tailoring of the functional properties of phase-change alloys. To this end, a thorough understanding of the microscopic features of phase-change materials is mandatory.

In this regard, atomistic simulations can provide valuable microscopic information that would be difficult to be gained experimentally. First-principles (or *ab initio*) electronic structure calculations are usually the tool of the trade, and

the field has greatly benefited from molecular dynamics (MD) simulations based on density functional theory (DFT).^{5,8,11–14}

Nonetheless, investigations of many properties of phase-change alloys lie well beyond the capabilities of DFT methods. For instance, the crystallization of amorphous nanowires (a possible alternative architecture for phase-change memories) requires simulations of $\sim 10^4$ atoms for several nanoseconds, while DFT simulations are typically limited to a few hundred atoms for up to few nanoseconds.

For a well-studied material such as silicon, it is straight-forward to perform large-scale simulations by picking an empirical/classical potential of choice and by striking some balance between accuracy (some of which would be lost) and computational efficiency. However, even though a classical interatomic potential has been devised for GeTe,¹⁵ phase-change materials display complex interplay between different atomic environments,¹⁶ which makes the construction of classical potentials challenging.

One way to solve this conundrum, where DFT is not fast enough, and classical potentials are not accurate enough, is to harness machine learning (ML) algorithms^{17–19} to build interatomic potentials with (*quasi*) *ab initio* accuracy and a computational efficiency (almost) comparable to that of classical potentials.

ML-based interatomic potentials

Machine learning (ML) is by now a pervasive aspect of technology that is percolating rapidly into many scientific fields. Materials science is no exception as ML may very well deliver the next generation of interatomic potentials for atomistic simulations. Actually, in this field ML algorithms are used as a flexible tool to build a potential energy surface by fitting a quite large data set (10^4 – 10^5 configurations) of DFT energies and forces of relatively small (10^2 atoms) configurations; two popular approaches in this context are based on Gaussian approximations²⁰ and neural networks (NNs).²¹

In the NN method of Behler and Parrinello,²¹ the structure of the system is encoded by means of so-called symmetry functions that describe the local atomic environment of each atom up to a cutoff radius typically encompassing up to the

third coordination shell. As depicted in **Figure 1a**, the symmetry functions represent the input of a feed-forward NN, which consists of a collection of nodes and layers where the inputs are subject to a nonlinear transformation (via so-called activation functions) and then are linearly combined via a number of “weights” to eventually yield the total energy of a given configuration. The weights are randomly initialized and then refined by back-propagation in order to minimize the mismatch between the energies predicted by the NN and by DFT.^{21,22} Once a sufficiently good fitting is achieved, we can leverage it to obtain the energy of very large models at low computational cost that scales linearly with the number of atoms. Crucially, forces and stress are readily available from NN potentials, thus enabling fast MD simulations while retaining an accuracy close to that of the underlying DFT calculations.

In the next sections, we illustrate how the neural network potential (NNP) for the prototypical phase-change compound GeTe that was generated in 2012²³ has allowed addressing several properties ranging from dynamical heterogeneity and fast crystallization in the liquid phase to structural relaxations in the amorphous phase.

Functional properties of the phase-change material GeTe

A neural network potential for GeTe

The NNP for GeTe described in References 23 and 24 was constructed from the DFT energies of ~30,000 configurations containing 64 to 216 atoms. The potential was validated against DFT calculations (an example is illustrated in Figure 1b) and it is capable of describing the bulk phases of GeTe as well as surfaces, nanowires, and nanoparticles. As a first application, the NNP was used to compute the thermal conductivity of the amorphous phase²⁵ and the thermal-boundary resistance at the amorphous-crystalline interface.²⁶ On this topic, the reader is referred to a recent review on the thermal properties of amorphous materials studied by means of ML potentials.²⁷

Fragility of supercooled liquid and structural relaxations in glass

In phase-change memories, crystallization of the amorphous phase is achieved by electrical pulses that bring the material to a supercooled liquid state above the glass-transition temperature T_g . One of the key properties of phase-change materials is that they tend to be fragile liquids,²⁸ which means that their viscosity (η) remains fairly low at large supercooling, only to rise sharply very close to T_g . This feature allows atoms to remain highly mobile at low temperatures (T), albeit above T_g , where the thermodynamical driving force for crystal nucleation and growth is also high.²⁸ The NNP developed in Reference 23 allowed²⁹ the function $\eta(T)$ to be computed, providing an estimate of the so-called fragility index (the slope of $\eta(T)$ at T_g) which turned out to be in reasonable agreement with later experimental data from ultrafast differential scanning calorimetry.²⁸

The atomic mobility at low T is further enhanced by a breakdown of the Stokes–Einstein relation between viscosity and diffusivity that was also predicted by MD simulations.²⁹ This feature is typical of fragile liquids and is often ascribed to the emergence of dynamical heterogeneities consisting of spatially separated domains in which atoms move substantially faster or slower than average. This is illustrated in **Figure 2a**. Close to the melting temperature, the distinction between slow (blue) and fast (red) moving regions is minimal. However, as the system is cooled down, one can clearly notice the emergence of spatially localized domains (Figure 2b).³⁰ These results were obtained by the so-called isoconfigurational analysis technique, which involves a large number (~ 100) of MD simulations.³⁰

Most notably, it turns out that fast-moving regions involve structural heterogeneities in the form of chains of Ge–Ge bonds, depicted in Figure 2c. These chains are ultimately responsible for the breakdown of the Stokes–Einstein relation and thus for an enhancement of atomic mobility at high supercooling which boosts the crystallization speed. They also play a role in the so-called resistance drift - a practical issue for phase-change memories whereby the resistance of the amorphous phase increases over time due to aging. In fact, by combining NNP and DFT calculations, it was found that Ge–Ge chains are responsible for localized electronic states within the gap of the amorphous

phase.³¹ Removal of these chains via structural relaxations over time (aging) leads to an energy gain and to a widening of the bandgap,³¹ which can explain the resistance drift (see Reference 32 for a review). Moreover, it was recently shown that the presence of Ge–Ge chains provides a rationale for the experimentally measured reduction of the resistance drift in GeTe nanowires,²⁴ whose amorphous structure is characterized, on average, by a lower fraction of Ge–Ge chains compared to the bulk.

Crystal nucleation and growth

The short time-scale of crystal nucleation and growth of phase-change materials offers the unique opportunity for DFT methods to study the crystallization process by means of unbiased MD simulations with an affordable computational load.³³ Indeed, this has been achieved in several works,^{12,34} but the usage of still relatively small models inevitably leads to spurious interactions between the newborn crystalline nuclei and their periodic images, thus affecting both induction times and crystal growth velocities.

The advent of NNP was a game changer in this respect, as it allowed the extent of finite size effects to be assessed (they are avoidable by using supercells containing at least about 1000 atoms) and to investigate crystal nucleation and growth in a wide range of conditions for supercells containing 4,000–32,000 atoms.^{35–37} Some of these findings are summarized in **Figure 3**. It was possible to identify different nucleation regimes at different temperatures (Figure 3a) and to accurately estimate the crystal growth velocity, extracted from the slope of growth profiles (Figure 3b). Recently, these growth rates were compared with those obtained for GeTe nanowires²⁴ (Figure 3c), which enabled the study of the effects of nanostructuring on crystallization kinetics.

Heterogeneous growth of crystalline GeTe,³⁷ a scenario of utmost relevance for phase-change memories, was also addressed by using large models of polycrystalline GeTe that allowed following the competition between the growth of different grains (Figure 3d). Moreover, simulations of the crystallization of the most studied ternary compound Ge₂Sb₂Te₅ have been performed very recently by means of a ML-based interatomic potential³⁸ based on

Gaussian approximations (the so-called GAP approach²⁰): a representative result is reported in Figure 3e.

Conclusions

Although DFT simulations have provided invaluable contributions to the study of phase-change materials, there is the need to bring MD simulations closer to the size scale of real memories in order to address key issues for the improvement of devices. ML-based interatomic potentials represent an effective solution, in that they can overcome the limitations of DFT calculations in terms of size and simulation time while keeping a *quasi-ab initio* accuracy.

In this article, we have illustrated some of the results obtained by means of a NNP for GeTe. The methodologies needed to construct ML potentials are now more accessible than they were in 2012 when the GeTe potential was devised. While a substantial effort is still needed to collect the huge data set of DFT energies, several promising advances,^{39,40} including stratified⁴¹ and implanted⁴² NN are now available to tackle multicomponent alloys.⁴³

There remain open questions in the field of phase-change memories that would greatly benefit from large-scale simulations of multicomponent alloys such as the switching mechanism of Ge-rich alloys for automotive applications⁴⁴ and of superlattices/interfacial phase-change memories.⁴⁵ For the hotly debated switching mechanism of interfacial phase-change memories,⁴⁶ DFT simulations have provided a number of different scenarios among which large-scale simulations might ultimately be able to identify the most plausible one. The impact of confinement effects and nanostructuring on crystallization kinetics is another issue where ML potentials can make a difference. Our previous work on GeTe nanowires is an example, but much remains to be explored, such as the fascinating possibility of monoatomic phase-change memories⁴⁷ or phase-change materials encapsulated in carbon nanotubes,⁴⁸ or even as isolated nanoparticles.⁴⁹

Besides the generation of interatomic potentials, ML and in particular NNs have been exploited very recently to predict glass properties by learning from existing experimental database.⁵⁰⁻⁵⁴ There are still relatively few examples of this type of application of ML in glass science, and none so far for tellurides of

interest for phase-change memories. However, the field is rapidly evolving and the growth of available data on phase-change alloys from both experiments and MD simulations could trigger the harnessing of ML to optimize alloys composition for tailored applications by learning from databases of physical properties.

In conclusion, in light of what the community has achieved in the last few years, we feel that ML can truly contribute to the rational design of phase-change materials for memories and other applications in the near future.

Acknowledgments

We acknowledge the contributions of several coworkers and in particular of J. Behler, who introduced us to the use of NN methods.

References

1. A. Pirovano, A.L. Lacaita, A. Benvenuti, F. Pellizzer, R. Bez, *IEEE Trans. Electron Devices* **51**, 452 (2004).
2. A.L. Lacaita, A. Redaelli, *Microelectron. Eng.* **109**, 351 (2013).
3. J. Choe, *TechInsights* (2017), <http://www.techinsights.com/about-techinsights/overview/blog/intel-3D-xpoint-memory-die-removed-from-intel-optane-pcm>.
4. M. Wuttig, N. Yamada, *Nat. Mater.* **6**, 824 (2007).
5. D. Lencer, M. Salinga, M. Wuttig, *Adv. Mater.* **23**, 2030 (2011).
6. W. Kim, M. BrightSky, T. Masuda, N. Sosa, S. Kim, R. Bruce, F. Carta, G. Fraczak, H.-Y. Cheng, A. Ray, Y. Zhu, H. L. Lung, K. Suu, and C. Lam, in *Proceedings of the 2016 IEEE International Electron Devices Meeting (IEDM), San Francisco, CA, 3-7 December 2016* (IEEE, 2016), pp. 83–86.
7. W. Kim et al., this issue.
8. F. Rao, K. Ding, Y. Zhou, Y. Zheng, M. Xia, S. Lv, Z. Song, S. Feng, I. Ronneberger, R. Mazzarello, W. Zhang, E. Ma, *Science* **358**, 1423 (2017).
9. G.W. Burr, R. M. Shelby, A. Sebastian, S. Kim, S. Kim, S. Sidler, K. Virwani, M. Ishii, P. Narayanan, A. Fumarola, L. L. Sanches, I. Boybat, M. Le Gallo, K. Moon, J. Woo, H. Hwang, Y. Leblebici, *Adv. Phys. X* **2**, 89 (2016).

10. M. Wuttig, H. Bhaskaran, T. Taubner, *Nat. Photonics* **11**, 465 (2017).
11. S. Caravati, M. Bernasconi, T.D. Kühne, M. Krack, M. Parrinello, *Appl. Phys. Lett.* **91**, 171906 (2007).
12. J. Hegedüs, S.R. Elliott, *Nat. Mater.* **7**, 399 (2008).
13. J. Akola, R.O. Jones, *Phys. Rev. B* **76**, 235201 (2007).
14. W. Zhang, V. L. Deringer, R. Dronskowski, R. Mazzarello, E. Ma, M. Wuttig, *MRS Bulletin* **40**, 856 (2015).
15. F. Zipoli, A. Curioni, *New J. Phys.* **15**, 123006 (2013).
16. V.L Deringer, R. Dobronowski, W. Muttig, *Adv. Funct. Mat.* **25**, 6343 (2015).
17. J. Behler, *J. Chem. Phys.* **145**, 170901 (2016).
18. A.P. Bartók, S. De, C. Poelking, N. Bernstein, J. R. Kermode, G. Csányi, M. Ceriotti, *Sci. Adv.* **3**, e1701816 (2017).
19. M.I. Jordan, T.M. Mitchell, *Science* **349**, 255 (2015).
20. A.P. Bartók, G. Csányi, *Int. J. Quantum Chem.* **115**, 1051 (2015).
21. J. Behler, M. Parrinello, *Phys. Rev. Lett.* **98**, 146401 (2007).
22. J. Behler, *Ang. Chem. Int. Ed.* **56**, 12828 (2017).
23. G.C. Sosso, G. Miceli, S. Caravati, J. Behler, M. Bernasconi, *Phys. Rev. B* **85**, 174103 (2012).
24. S. Gabardi, E. Baldi, E. Bosoni, D. Campi, S. Caravati, G. C. Sosso, J. Behler, and M. Bernasconi, *J. Phys. Chem. C* **121**, 23827 (2017).
25. G.C. Sosso, D. Donadio, S. Caravati, J. Behler, M. Bernasconi, *Phys. Rev. B* **86**, 104301 (2012).
26. D. Campi, D. Donadio, G.C. Sosso, J. Behler, M. Bernasconi, *J. Appl. Phys.* **117**, 015304 (2015).
27. G.C. Sosso, V.L. Deringer, S.R. Elliott, G. Csányi, *Mol. Simul.* **44**, 866 (2018).
28. H. Weber, J. Orava, I. Kaban, J. Pries, A.L. Greer, *Phys. Rev. Mater.* **2**, 093405 (2018).
29. G.C. Sosso, J. Behler, M. Bernasconi, *Phys. Status Solidi B* **249**, 1880 (2012).

30. G.C. Sosso, J. Colombo, J. Behler, E. Del Gado, M. Bernasconi, *J. Phys. Chem. B* **118**, 13621 (2014).
31. S. Gabardi, S. Caravati, G.C. Sosso, J. Behler, M. Bernasconi, *Phys. Rev. B* **92**, 054201 (2015).
32. J.-Y. Raty, *Phys. Status Solidi RRL* **13**, 1800590 (2019).
33. G.C. Sosso, J. Chen, S. J. Cox, M. Fitzner, P. Pedevilla, A. Zen, A. Michaelides, *Chem. Rev.* **116**, 7078 (2016).
34. W. Zhang, R. Mazzarello, M. Wuttig, E. Ma, *Nat. Rev. Mater.* **4**, 150 (2019).
35. G.C. Sosso, G. Miceli, S. Caravati, F. Giberti, J. Behler, and M. Bernasconi, *J. Phys. Chem. Lett.* **4**, 4241 (2013).
36. S. Gabardi, G. C. Sosso, J. Behler, and M. Bernasconi *Faraday Discuss.* **213**, 287 (2019).
37. G.C. Sosso, M. Salvalaglio, J. Behler, M. Bernasconi, M. Parrinello, *J. Phys. Chem. C* **119**, 6428 (2015).
38. F.C. Mocanu, G. Csányi, and S. R. Elliott, *J. Phys. Chem. B* **122**, 8998 (2018).
39. H. Chan, B. Narayanan, M. J. Cherukara, F. G. Sen, K. Sasikumar, S. K. Gray, M. K. Y. Chan, S. K. R. S. Sankaranarayanan, *J. Phys. Chem. C* **123**, 6941 (2019).
40. L. Zhang, D.-Y. Lin, H. Wang, R. Car, W. E, *Phys. Rev. Mater.* **3**, 023804 (2019).
41. S. Hajinazar, J. Shao, A.N. Kolmogorov, *Phys. Rev. B* **95**, 014114 (2017).
42. B. Onat, E.D. Cubuk, B.D. Malone, E. Kaxiras, *Phys. Rev. B* **97**, 094106 (2018).
43. R. Kobayashi, D. Giofré, T. Junge, M. Ceriotti, W.A. Curtin, *Phys. Rev. Mater.* **1**, 053604 (2017).
44. E. Palumbo, P. Zuliani, M. Borghi, R. Annunziata, *Solid State Electron.* **133**, 38 (2017).
45. R.E. Simpson, P. Fons, A.V. Kolobov, T. Fukaya, M. Krbal, T. Yagi, J. Tominaga, *Nat. Nanotechnol.* **6**, 501 (2011).
46. M. Boniardi, J. E. Boschker, J. Momand, B. J. Kooi, A. Redaelli, and R. Calarco, *Phys. Status Solidi (RRL)* **13**, 1800634 (2019).

47. M. Salinga, B. Kersting, I. Ronneberger, V. P. Jonnalagadda, X. T. Vu, M. Le Gallo, I. Giannopoulos, O. Cojocar-Mirédin, R. Mazzarello, A. Sebastian, *Nat. Mater.* **17**, 681 (2018).
48. J.M. Wynn, P. V. C. Medeiros, A. Vasylenko, J. Sloan, D. Quigley, A. J. Morris, *Phys. Rev. Mater.* **1**, 073001 (2017).
49. B. Chen, G.H. ten Brink, G. Palasantzas, B.J. Kooi, *Sci. Rep.* **6**, 39546 (2016).
50. D. R. Cassar, A. C. P. L. F. de Carvalho, E. D. Zanotto, *Acta Mater.* **159**, 249 (2018).
51. C. Dreyfus, G. A Dreyfus, *J. Non-Cryst. Solids* **318**, 63 (2003). ^[1]_{SEP}
52. N. M. A. Krishnana, S. Mangalathub, M. M. Smedskjaerc, A. Tandiad, H. Burtonb, M. Bauchy, *J. Non-Cryst. Solids* **487**, 37 (2018). ^[1]_{SEP}
53. L. Ward, S. C. O'Keeffe, J. Stevick, G. R. Jelbert, M. Aykol, C. Wolverton, *Acta Mater.* **159**, 102 (2018).
54. M.C. Onbaşı, A. Tandia, J.C. Mauro, Mechanical and Compositional Design of High-Strength Corning Gorilla® Glass. In: W. Andreoni, S. Yip (eds) *Handbook of Materials Modeling*, Springer, (2018).

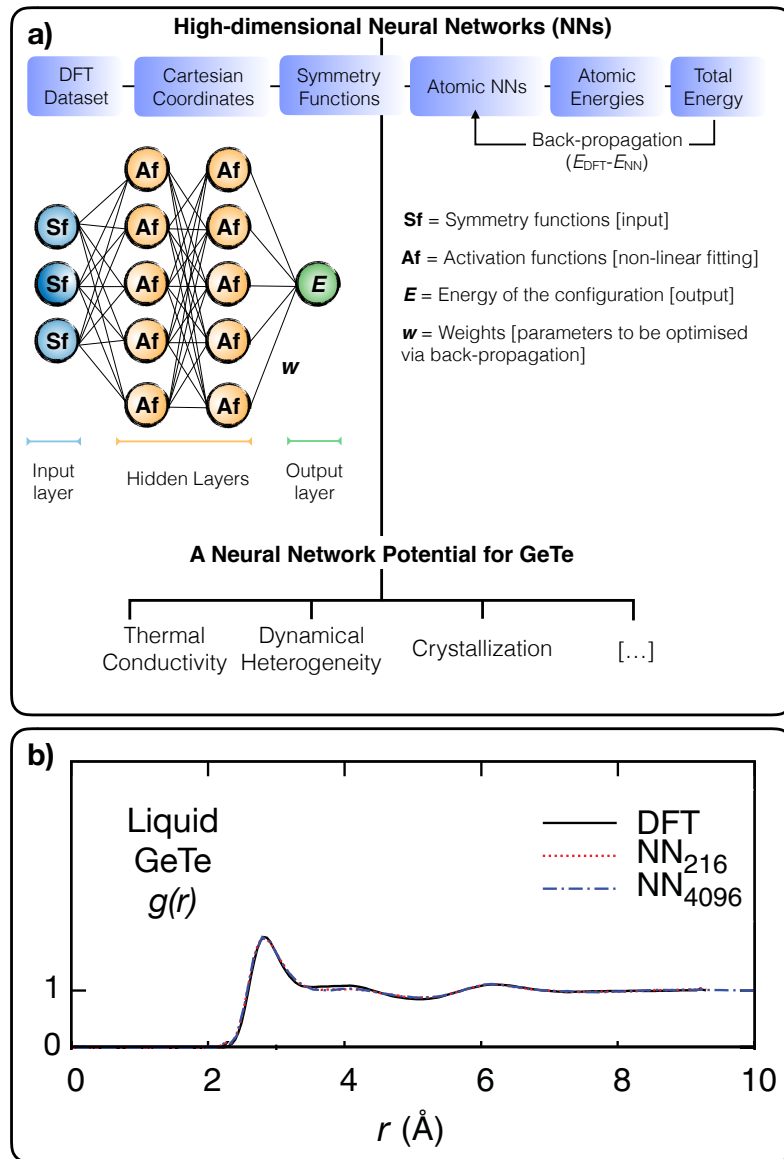


Figure 1. (a) Neural networks (NN) can be harnessed to construct a machine learning (ML)-based interatomic potential starting from a data set of density functional theory (DFT) energies of small (100 atoms) configurations. The weights w of the NN are assigned by back-propagation which is a procedure aimed at minimizing the mismatch between the energy predicted by the NN (E_{NN}) and the DFT energies (E_{DFT}). (b) Total pair correlation function, $g(r)$, of liquid GeTe from a NN simulation with 4096 and 216 atoms, compared with DFT results for the smaller cell. The $g(r)$ gives a measure of the probability to find an atom at a distance r from an atom set at the origin. Adapted with permission from Reference 23. © 2012 American Physical Society.

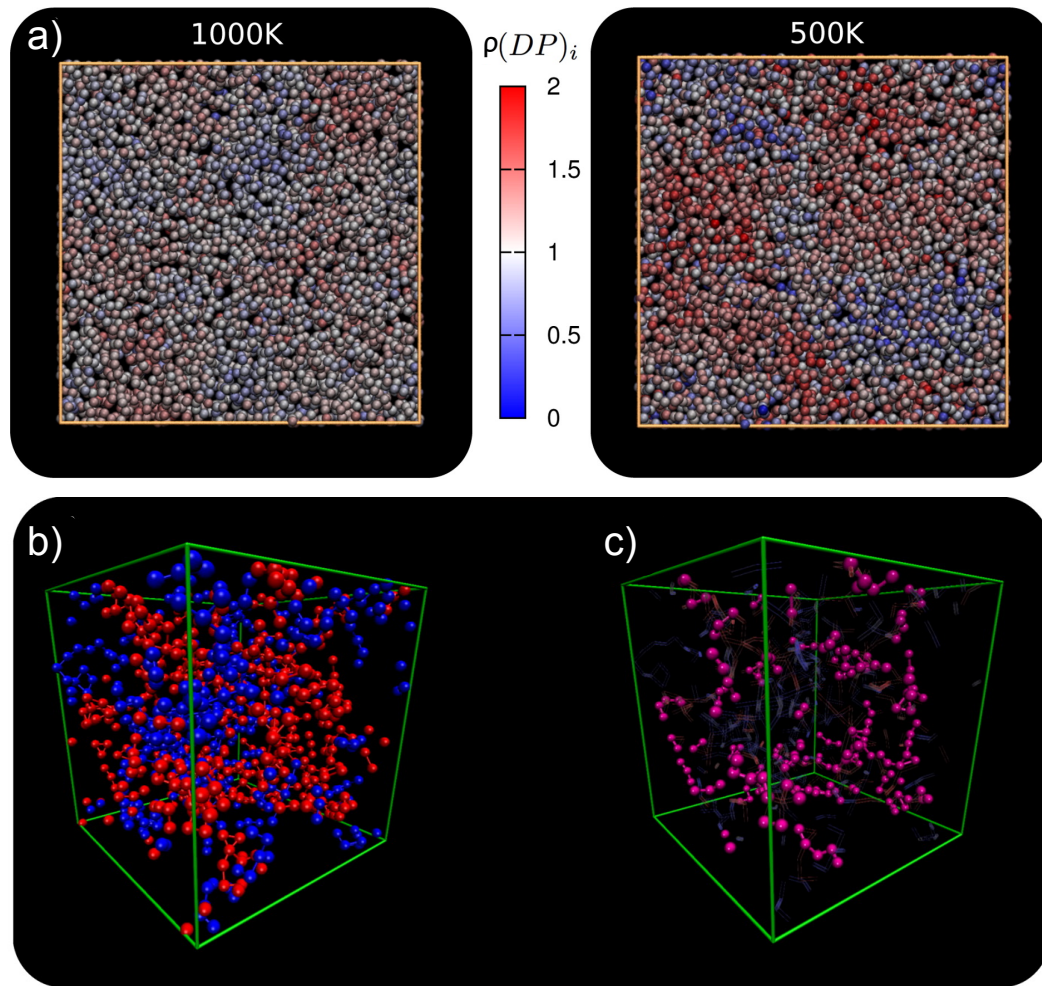


Figure 2. Dynamical heterogeneity in liquid GeTe from MD simulations employing a NNP. (a) The colour map refers to the density ρ of the dynamical propensity (DP), calculated according to Eq. 4 in Reference 30. Slow- and fast-moving domains are highlighted in blue and red, respectively. (b) Spatially localized clusters of slow- and fast-moving atoms at 500 K. Chains of Ge–Ge bonds found in most mobile regions (purple) are highlighted in (c). Adapted with permission from Reference 30. © 2014 American Physical Society.

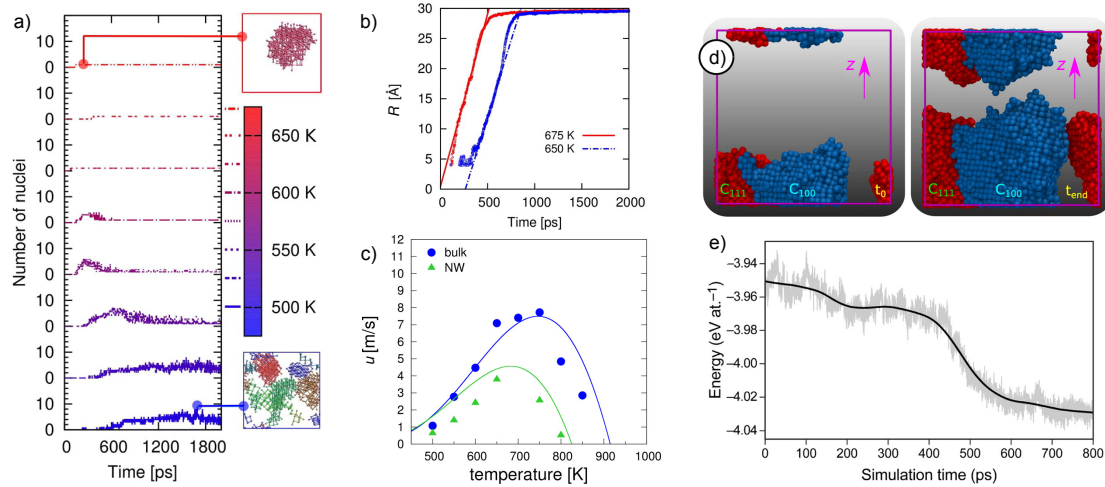


Figure 3. (a)-(d) Results on the crystallization of GeTe from MD simulations using a NNP. (a) Number of crystalline nuclei (>29 atoms) at different temperatures as a function of time in supercooled liquid GeTe. The number of nuclei first increases and then decreases due to coalescence. The two snapshots (*insets* at the top and bottom) show crystalline atoms forming a single nucleus or several nuclei at high and low temperatures respectively. (b) The radius, R , of a crystalline nucleus of GeTe at two temperatures as a function of time. Reprinted with permission from Reference 35. © 2013 American Chemical Society. (c) Crystal growth velocity, U , of a GeTe nanowire (NW, green triangles) and at the crystal/liquid interface in the bulk (blue circles). Reprinted with permission from Reference 24. © 2017 American Chemical Society. (d) C_{111} (red) and C_{100} (blue) crystalline grains in a polycrystalline model of GeTe at the beginning (t_0) and end (t_{end}) of the simulation. Projections along the xz planes are shown. Reprinted with permission from Reference 37. © 2015 American Chemical Society. (e) Potential energy as a function of time in the simulation of the crystallization of $Ge_2Sb_2Te_5$ with a Gaussian approximation potential. Reprinted with permission from Reference 38. © 2018 American Chemical Society.

Gabriele C. Sosso is an assistant professor of computational physical chemistry at the University of Warwick, UK. He earned the MS in Materials Science at the University of Milano-Bicocca, Italy, in 2009 and the PhD degree in Nanostructures and Nanotechnologies from the same institution in 2013. He held postdoctoral positions at ETH Zurich, Switzerland, and at the University College London UK. His research includes disordered systems and phase transitions, focusing on crystal nucleation and growth. Sosso can be reached via email at g.sosso@warwick.ac.uk.

Marco Bernasconi is a full professor of theoretical condensed-matter physics and dean of the Doctorate School in Materials Science and Nanotechnology at the University of Milano-Bicocca, Italy. He received his PhD degree in physics from Sissa-Trieste in 1993. After several years at the Max-Planck-Institut, Germany, he moved to Milano-Bicocca in 1998. His research focuses on electronic structure calculations and molecular dynamics simulations of materials for applications in microelectronics and photonics. Bernasconi can be reached by email at marco.bernasconi@unimib.it.